

Effects of coastal managed retreat on mercury biogeochemistry

Article

Accepted Version

Sizmur, T. ORCID: <https://orcid.org/0000-0001-9835-7195>, Godfrey, A. and O'Driscoll, N. J. (2016) Effects of coastal managed retreat on mercury biogeochemistry. *Environmental Pollution*, 209. pp. 99-106. ISSN 0269-7491 doi: <https://doi.org/10.1016/j.envpol.2015.11.016> Available at <https://centaur.reading.ac.uk/48003/>

It is advisable to refer to the publisher's version if you intend to cite from the work. See [Guidance on citing](#).

To link to this article DOI: <http://dx.doi.org/10.1016/j.envpol.2015.11.016>

Publisher: Elsevier

All outputs in CentAUR are protected by Intellectual Property Rights law, including copyright law. Copyright and IPR is retained by the creators or other copyright holders. Terms and conditions for use of this material are defined in the [End User Agreement](#).

www.reading.ac.uk/centaur

CentAUR

Central Archive at the University of Reading

Reading's research outputs online



1 Effects of coastal managed retreat on mercury biogeochemistry

2

3 Tom Sizmur^{a*}, Adam Godfrey^a and Nelson J. O'Driscoll^a

4

5 ^aDepartment of Earth & Environmental Science, K.C. Irving Environmental Science Center,
6 Acadia University, Wolfville, NS, B4P 2R6, Canada.

7

8 *Corresponding author

9 Present address: Soil Research Centre, Department of Geography and Environmental Science,
10 Russell Building, University of Reading, Reading, RG6 6DW, UK

11 E-mail: t.sizmur@reading.ac.uk

12 Phone: +44(0)118 3788913

13

14 **Abstract**

15 We investigated the impact of managed retreat on mercury (Hg) biogeochemistry at a site subject
16 to diffuse contamination with Hg. We collected sediment cores from an area of land behind a
17 dyke one year before and one year after it was intentionally breached. These sediments were
18 compared to those of an adjacent mudflat and a salt marsh. The concentration of total mercury
19 (THg) in the sediment doubled after the dyke was breached due to the deposition of fresh
20 sediment that had a smaller particle size, and higher pH. The concentration of methylmercury
21 (MeHg) was 27% lower in the sediments after the dyke was breached. We conclude that coastal
22 flooding during managed retreat of coastal flood defences at this site has not increased the risk of
23 Hg methylation or bioavailability during the first year. As the sediment becomes vegetated,
24 increased activity of Hg-methylating bacteria may accelerate Hg-methylation rate.

25 **Keywords:** Mercury, Methylmercury, Biogeochemistry, Sediment deposition, Coastal

26 **Capsule:** Mercury concentration doubled in sediments after coastal flooding but methylmercury
27 concentration decreased

28 **Introduction**

29 Coastal wetlands have been subject to dramatic global declines in the past due to dyking and
30 draining for agriculture. However, this practice is now being reversed in many countries because
31 salt marshes are valued as habitats for wildlife and as natural defence against rising sea-levels
32 (Singh et al., 2007). Managed retreat of coastal defences has led to an increase in the number of
33 sites where dykes are breached, agricultural fields are inundated with seawater, sediment is
34 deposited over soils, and new salt marshes are created. Inundation of previously dyked farmland
35 leads to considerable biogeochemical changes, characterised by increased salinity, lower redox
36 potential (Portnoy and Giblin, 1997) and a decaying mat of buried vegetation (Emmerson et al.,
37 2000). There is concern that biogeochemical changes during managed retreat may alter the fate
38 of redox-sensitive contaminants such as mercury (Hg) (Morris et al., 2014).

39

40 The Bay of Fundy in Southeastern Canada is renowned for having the largest tidal amplitude in
41 the world, which gives rise to expansive intertidal mudflats and vast areas of salt marsh (Crowell
42 et al., 2011; Desplanque and Mossman, 2004). For centuries the Bay's coastline has been
43 extensively dyked to use the land for agriculture (Wynn, 1979). The land surrounding the Bay of
44 Fundy is designated a 'biological mercury hotspot' due to elevated concentrations of Hg in biota
45 (Evers et al., 2007). The Bay of Fundy itself has been identified as an area of special concern for
46 Hg contamination because the Bay's ecosystem may be critical to concentrations of Hg found in
47 fish, birds and wildlife (Hung and Chmura, 2006).

48

49 Mercury enters the Bay of Fundy through seawater inflow and atmospheric deposition
50 (Sunderland et al., 2012). The Hg present in sediments of the Bay of Fundy is strongly
51 associated with organic matter and fine textured sediments (O'Driscoll et al., 2011; Sizmur et al.,
52 2013b). Inorganic Hg in sediments can be converted to methylmercury (MeHg) under anoxic
53 conditions by sulphate-reducing bacteria (Compeau and Bartha, 1985). Methylmercury can
54 biomagnify through food webs (Lavoie et al., 2010) and is a potent neurotoxin affecting higher
55 trophic level animals and humans (Rasmussen et al., 2005).

56

57 Increases in MeHg concentrations in sediments and biota have been observed during the decades
58 that follow terrestrial freshwater flooding for dam construction or wetland creation (Kelly et al.,
59 1997; Sinclair et al., 2012). However, little research has been done to assess changes in Hg
60 biogeochemistry after coastal wetland flooding. Terrestrial flooding events, like reservoir or
61 wetland creation, entail a permanent change in sediment redox from oxic to anoxic conditions
62 because the sediments are constantly flooded. However, coastal flooding events subject the land
63 to fluctuating oxic/anoxic conditions due to the tidal cycle. These fluctuations generate an oxic-
64 anoxic interface in the sediment. The temporal fluctuations in redox conditions increases the
65 volume of sediment where sulphate reduction and mercury methylation may occur (Heim et al.,
66 2007; Sizmur et al., 2013a). However, there is also frequent tidal flushing of inundated areas
67 which acts as a significant means of removing MeHg from the surface of coastal sediments
68 (Guédron et al., 2012). Therefore, it is not clear if managed retreat will increase or decrease Hg
69 and MeHg concentrations in sediments.

70

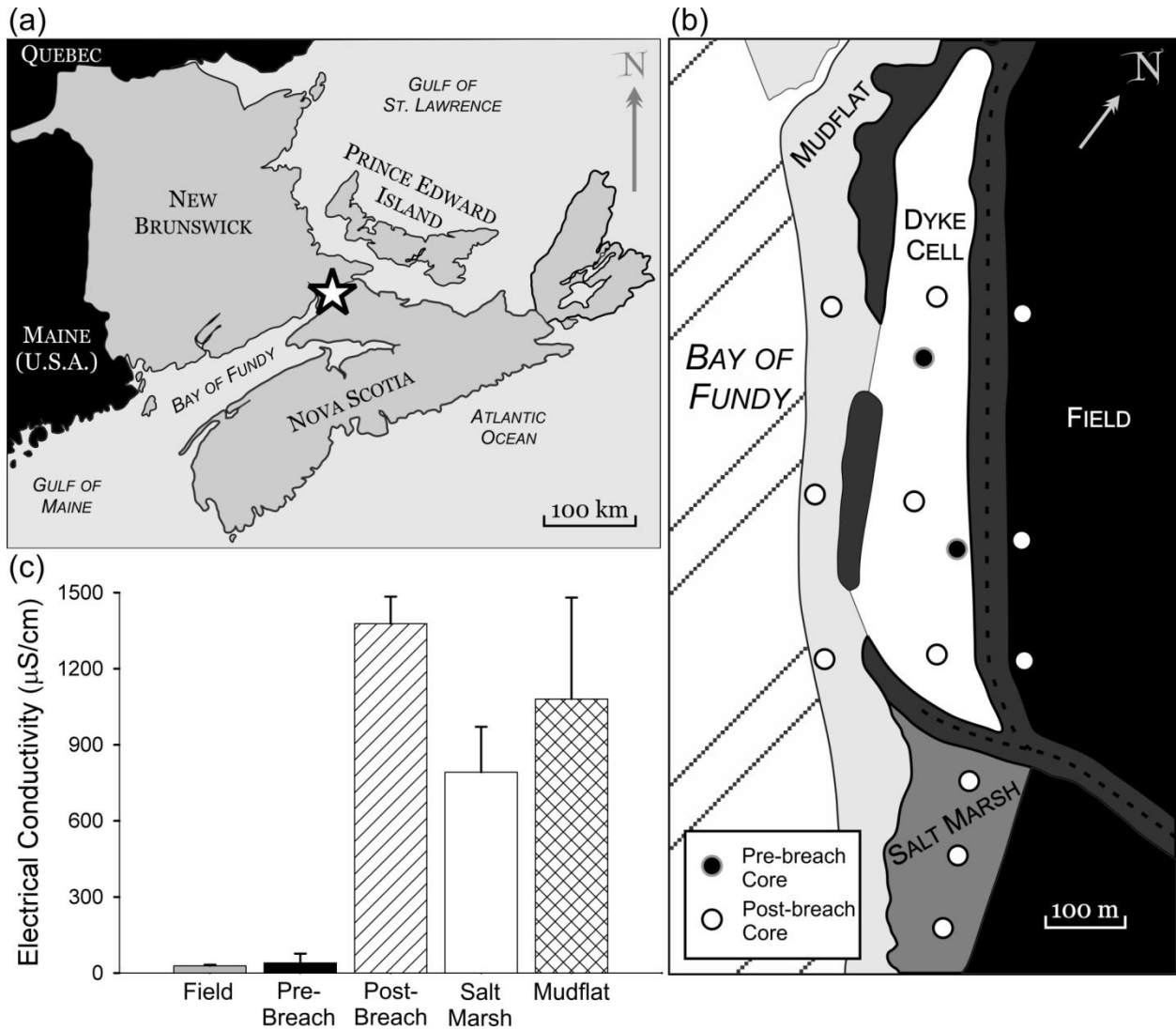
71 We investigated the effects of managed retreat on mercury biogeochemistry at Beaubassin
72 Research Station where a dyke has recently been breached, allowing the seawater to inundate
73 land previously drained for agriculture.

74

75 **Materials and Methods**

76 Site Description

77 Beaubassin Research Station (Latitude: 45.852195 Longitude: -64.279631) is located on the
78 Chignecto Isthmus between Nova Scotia and New Brunswick, Canada (Figure 1a). It lies along
79 the Cumberland Basin, a branch of Chignecto Bay, in the Bay of Fundy which is sourced from
80 the Gulf of Maine. The average tidal amplitude at Beaubassin is 11 m (Gordon Jr and Baretta,
81 1982). Recently, an eroding 150-year-old dyke was replaced with a new dyke built
82 approximately 90 m back from the pre-existing coastline in order to protect transport
83 infrastructure and the historic site of Fort Beausejour from tidal surges. The 40 ha of low lying
84 land between the old dyke and the new dyke (Latitude: 45.851595 Longitude: -64.294379) was
85 flooded in October 2010. Flooding occurred when the old dyke was deliberately breached so that
86 sediment could accumulate to protect the new dyke before the old dyke completely failed
87 (Ollerhead et al., 2011). Tidal re-entry has resulted in the rapid deposition of fresh sediment over
88 the top of the agricultural soil, burying a mat of terrestrial vegetation. At the time of sampling,
89 new salt marsh vegetation was yet to establish.



90

91 Figure 1. (a) Site location at Beaubassin, New Brunswick, Canada; (b) Location of all
 92 cores sampled from the dyke cell (pre-breach and post-breach) along with adjacent
 93 sites (mudflat, salt marsh and field). The location of two gaps in the wall of the dyke cell
 94 represent where they were deliberately breached in 2010; (c) Electrical conductivity of
 95 sediment cores sampled (averaged 0-15 cm) shown here to demonstrate the influence
 96 of seawater on the dyke cell pre-breach and post-breach.

97

98 Sample Collection and Preparation

99 Two 16 cm deep cores were taken in the dyke cell (Figure 1b) between the new and the old
100 dykes (hereafter referred to as the pre-breach cores) in summer 2009 (before the old dyke was
101 breached in 2010). We returned to the site in summer 2011 to collect cores one year after the old
102 dyke was breached. Three 15 cm deep cores were sampled at four locations: (i) The area
103 previously sampled in the dyke cell between the new and old dykes (hereafter referred to as the
104 post-breach cores), (ii) the mudflat seaward of the dyke cell, (iii) a pre-existing salt marsh
105 adjacent to the dyke cell, and (iv) the field landward of the dyke cell (Figure 1b). All cores were
106 sampled at low tide using polyvinyl chloride (PVC) cores (10 cm internal diameter) that were
107 dug out with a stainless steel spade.

108

109 Pre-breach cores were sliced in 2 cm intervals to a depth of 16 cm, producing a total of eight
110 slices per core. Each of the post-breach, mudflat, salt marsh, and field cores were sliced at 1 cm
111 intervals for the upper 5 cm of sediment and then at 2 cm intervals for the remaining 10 cm,
112 producing a total of 10 core slices per core. Core slices were individually sealed in Ziploc bags at
113 the research station and placed in a dark cooler with ice packs for transport back to the
114 laboratory.

115

116 At the laboratory each sediment slice was thoroughly homogenised by hand in the Ziploc bag
117 and frozen as a wet homogenate at -20 °C. Sediment samples were later thawed and a subsample
118 dried at 60 °C for 24 hours. Dried sediment samples were ground with a pestle and mortar and
119 sieved to < 2 mm. A subsample of wet sediment was analysed for electrical conductivity (EC)

120 using a VWR Symphony SP90M5 meter and Orion electrical conductivity probe. The field was
121 only sampled to demonstrate that the pre-breach sediments had not been inundated by seawater
122 prior to the breach. Since the EC of the pre-breach and field cores (Figure 1c) revealed no
123 significant difference ($p > 0.05$), further analysis of the field cores was deemed unnecessary.
124 Each slice of the remaining cores was analysed for total mercury (THg), MeHg, percentage
125 organic matter (%OM), particle size distribution, water-extractable organic carbon (WEOC) and
126 pH.

127

128 Analytical Procedures

129 Total mercury in sediment was determined using thermal degradation – gold amalgamation
130 atomic absorbance spectroscopy as outlined in EPA Method 7473 (1998) using a Nippon MA-
131 2000 non-dispersive double-beam cold-vapor atomic absorption Hg analyzer. Methylmercury
132 was determined in sediments by alkaline digestion, ethylation purge and trap Gas
133 Chromatography - Cold Vapour Atomic Fluorescence Spectrometry (GC-CVAFS) following
134 Sizmur et al (2013b). A 100 mg sample of sediment was digested in 2.5 ml of basic methanol (25
135 % KOH/MeOH) by shaking on a reciprocal shaker for 1 hour and then heating for 1 hour at 90
136 °C. Within 24 hours of digestion, a 60 µl aliquot was transferred to a glass reaction bubbler,
137 ethylated with $\text{NaB}(\text{C}_2\text{H}_5)_4$, purged with argon, collected on a Tenax trap and analysed for MeHg
138 using GC-AFS (Brooks Rand Model III).

139

140 Organic matter in sediment was determined by loss on ignition at 500 °C (Byers et al., 1978) and
141 particle size distribution by the micro-pipette method (Miller and Miller, 1987). Sand was

142 calculated as particles 2000-63 μm , silt as 63-2 μm , and clay as $< 2 \mu\text{m}$ in diameter. Water-
143 extractable organic carbon was determined following Sizmur et al (2011) by shaking 1 g of
144 sediment with 40 ml of Milli Q water for 2 hours on a reciprocal shaker at 120 shakes min^{-1} ,
145 followed by centrifuging at 4000 rpm (2647 G) for 20 min and filtering to $< 0.45 \mu\text{m}$ with
146 polypropylene membrane filters, before TOC/TIC analysis with a Shimadzu TOC-V CPH Total
147 Organic Carbon Analyzer. Sediment pH was analysed in WEOC vials prior to centrifuging.

148

149 Quality control

150 Sediments were analysed in triplicate alongside certified reference materials MESS-3 (National
151 Research Council Canada) and SQC-1238 (Sigma Aldrich RTC) for THg and MeHg
152 respectively. Mean recovery of THg from MESS-3 was 102.2 % (SD = 1.4 %). Mean recovery of
153 MeHg from SQC-1238 was 94.4 % (SD = 12.0 %). Detection limits for MeHg and THg were
154 0.65 and 1.21 pmol g^{-1} , respectively. Both samples and reference materials during Hg analysis
155 were corrected for background by subtracting averaged method blanks from the analysed
156 samples.

157 Statistical Analysis

158 Statistical analysis was carried out using Genstat version 16. Normality and homoscedasticity
159 was assessed by inspecting residual plots. Two-way analysis of variance was carried out on all
160 data (MeHg, THg, pH, clay, %OM, WEOC and EC) using 'site' and 'depth' as the factors and
161 allowing for interactions. Fisher's least significant difference was used to identify differences
162 between individual treatments. Multiple linear regression was carried out by forward selection;
163 first the variable that resulted in the highest R^2 values was included in the model, then variables

164 that resulted in the greatest increase were added. Data presented in text as average values at each
 165 site are calculated from the concentrations in cores averaged across all depths. All the raw data is
 166 provided in the supporting information.

167

168 **Results**

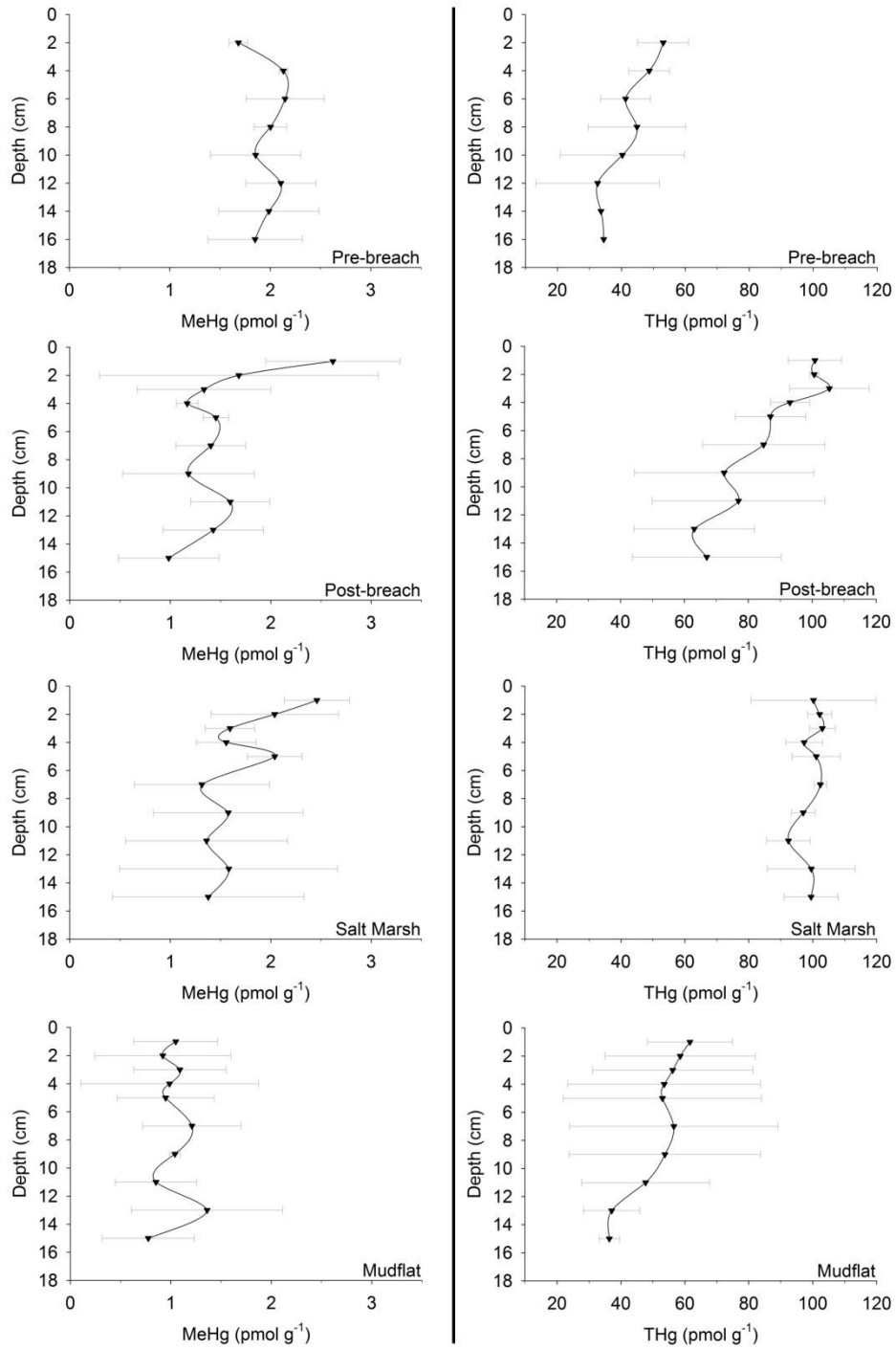
169 Mercury and Methylmercury

170 The average concentration of THg in the post-breach cores was 85.1 pmol g⁻¹ (SD = 15.6) which
 171 was approximately double the concentration in the pre-breach cores (41.1 pmol g⁻¹, SD = 9.52).
 172 THg decreased significantly (p < 0.001) with depth (Table 1) in the post-breach and mudflat
 173 cores but this decrease was not observed in the pre-breach or the salt marsh cores (Figure 2). The
 174 THg concentration in the salt marsh cores was significantly (p < 0.05) greater than the mudflat or
 175 the dyke cell pre- or post-breach. The post-breach cores had significantly (p < 0.05) greater Hg
 176 concentrations than the pre-breach cores.

177 Table 1 Analysis of variance from physiochemical sediment variables; Water Extractable
 178 Organic Carbon (WEOC), pH, Electrical Conductivity (EC), Clay content and Organic Matter
 179 (OM).

Variable	Site F value	Depth F value	Site-depth interaction F value
THg	62.19***	2.34*	0.41
MeHg	12.83***	2.06*	0.55
% MeHg	31.41***	0.95*	0.62
% OM	15.03***	0.29	0.93
pH	16.87***	0.97*	0.79
% Clay	24.93***	1.74	0.38
WEOC	32.14***	1.68	1.36
EC	69.15***	0.82	1.23

180 * = p < 0.05, *** = p < 0.001



181

182 Figure 2. Total mercury (THg) and methylmercury (MeHg) concentrations of sediment
 183 slices of cores sampled from the dyke cell (pre-breach and post-breach) along with
 184 adjacent sites (mudflat and salt marsh). The error bars represent the standard deviation
 185 of three replicate cores (n = 2 for the pre-breach cores).

186 MeHg significantly ($p < 0.05$) decreased with depth (Table 1) in the post-breach and salt marsh
187 cores (Figure 2). Although THg was greater after inundation, MeHg concentration was
188 significantly ($p < 0.05$) lower in post-breach sediments (Figure 2). Methylmercury
189 concentrations were 27% lower in the post-breach cores (1.48 pmol g^{-1} , $SD = 0.54$) compared to
190 the pre-breach cores (1.97 pmol g^{-1} , $SD = 0.31$). However, we did measure 36% higher MeHg
191 concentrations in the upper 2 cm of the post-breach sediment than in the top 2 cm of the pre-
192 breach cores (Figure 2). The post-breach MeHg concentration was not significantly ($p > 0.05$)
193 different than that measured in the salt marsh (1.69 pmol g^{-1} , $SD = 0.60$) but was significantly (p
194 > 0.05) greater than MeHg in the mudflat (1.02 pmol g^{-1} , $SD = 0.51$). The percentage of MeHg
195 as a proportion of the THg (%MeHg) was significantly ($p < 0.05$) greater in the pre-breach cores
196 (5.97% , $SD = 2.99$) than the post-breach cores (2.02% , $SD = 0.58$). %MeHg in the post-breach
197 sediment was not significantly ($p > 0.05$) different from the mudflat (2.34%) or salt marsh
198 (1.84%) sediments.

199

200 *Physiochemical variables*

201 The EC of the pre-breach cores was not significantly different to the samples taken from the field
202 behind the new dyke. EC was significantly increased ($p < 0.05$) by periodic tidal inundation of
203 the dyke cell, increasing over 2000% from pre- to post-breach (Figure 1c). Post-breach sediment
204 EC was also significantly ($p < 0.05$) greater than the salt marsh and mudflat but the magnitude of
205 the difference was much smaller.

206

207 Sediment pH was significantly ($p < 0.001$) greater after inundation of the dyke cell, rising from
208 5.08 ($SD = 1.2$) in the pre-breach cores to 7.43 ($SD = 0.6$) in the post-breach cores (Figure 3).

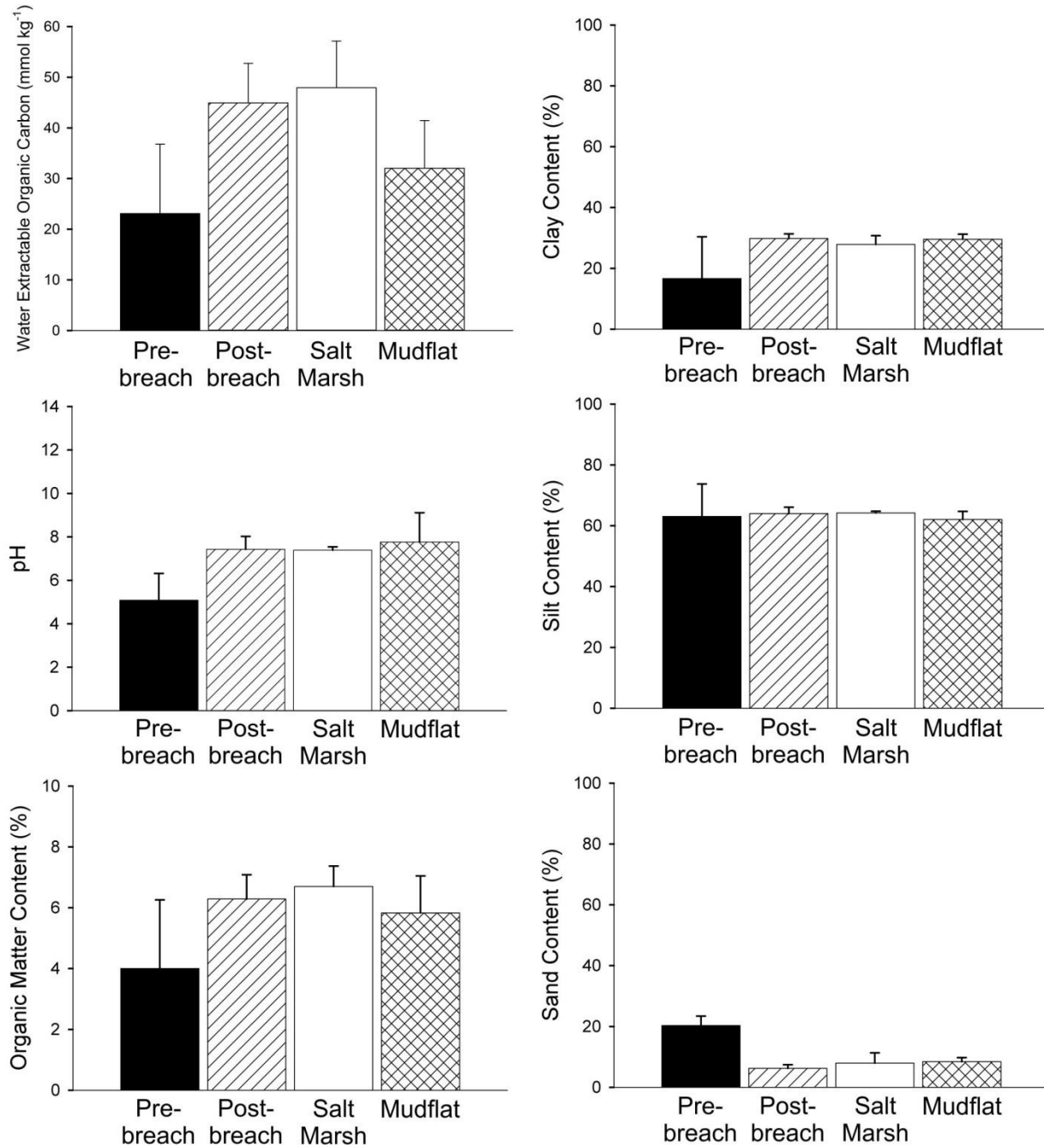
209 There was no significant ($p > 0.05$) pH difference between the post-breach cores and the salt
210 marsh or mudflat cores.

211

212 The texture of the sediment in the top 15 cm of the dyke cell significantly ($p < 0.001$) changed
213 during salt marsh restoration as fresh sediment with a smaller particle size distribution was
214 deposited over the top of the drained agricultural field (Figure 3). Percentage clay was
215 significantly ($p < 0.05$) greater and sand significantly ($p < 0.05$) lower in the sediment after the
216 inundation. Percentage clay in the post-breach cores (29.8%, SD = 1.52) was nearly double that
217 in the pre-breach cores (16.6%, SD = 13.8). The proportions of sand, silt and clay in the post-
218 breach cores were not significantly ($p > 0.05$) different to the sediments sampled from the
219 mudflat (Figure 3) but clay content was significantly ($p < 0.05$) greater than sediments sampled
220 from the salt marsh.

221

222 The post-breach sediments had significantly ($p < 0.05$) higher organic matter (%OM) and WEOC
223 than the pre-breach cores (Table 1 and Figure 3). There was no significant ($p > 0.05$) difference
224 between the post-breach cores and the salt marsh and mudflat cores, for either %OM or WEOC.
225 The concentration of both WEOC ($44.9 \text{ mmol kg}^{-1}$, SD = 4.64) and %OM (6.3%, SD = 0.8) in
226 the post-breach cores was greater than the mudflat cores ($32.1 \text{ mmol kg}^{-1}$, SD = 8.87 and 5.8%,
227 SD = 1.2) but lower than the salt marsh cores ($47.9 \text{ mmol kg}^{-1}$, SD = 7.17 and 6.7%, SD = 0.7).



228

229 Figure 3. Physiochemical variables measured in cores (averaged 0-15 cm) sampled
 230 from the dyke cell (pre-breach and post-breach) along with adjacent sites (mudflat and
 231 salt marsh). The error bars represent standard deviation of three replicate cores (n = 2
 232 for the pre-breach cores).

233

234 Multiple linear regressions

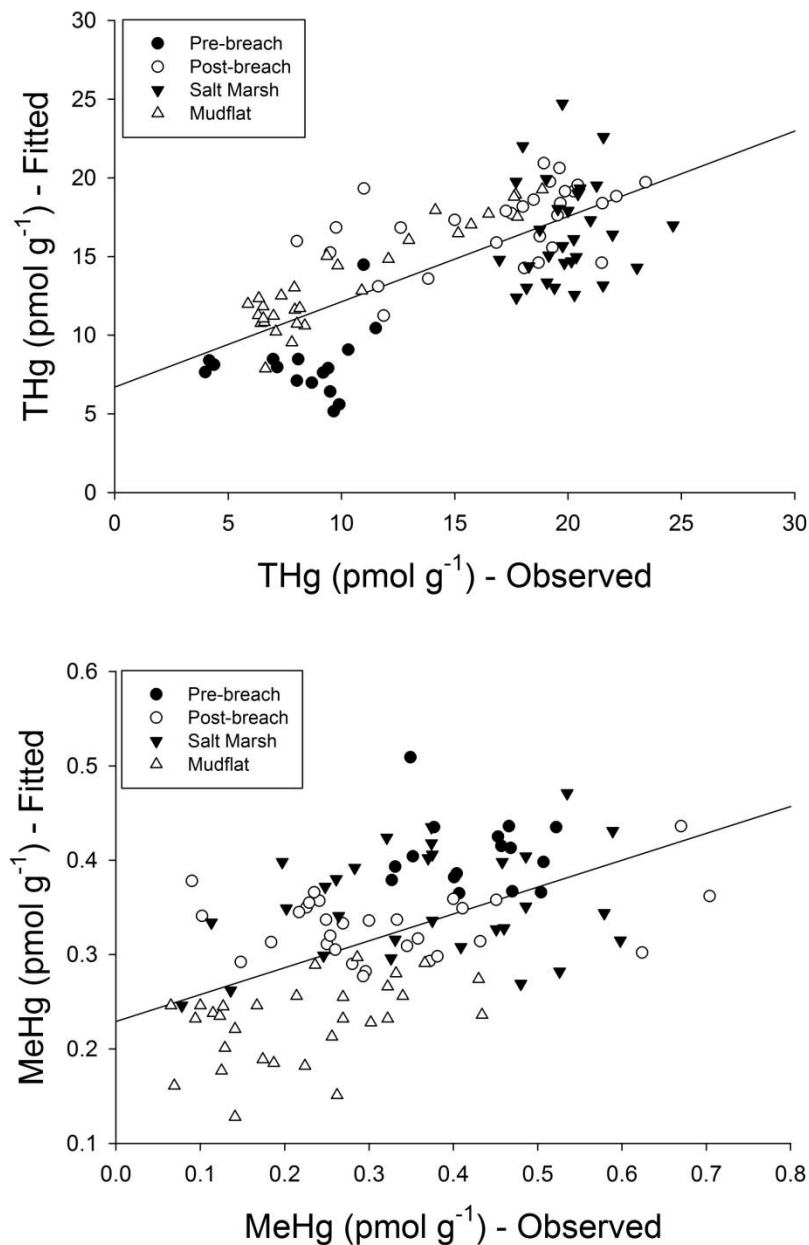
235 The correlation between the best multiple linear regression model and the THg concentrations
 236 measured in the sediments (Figure 4) yielded an R² value of 0.524 and a p value < 0.001 (Table
 237 2). The explanatory variables in order of decreasing importance were WEOC, pH, EC and
 238 %Clay. Adding the next most important variable (%OM) decreased the R² value to 0.519.
 239 WEOC alone explained 36.7% of the variation in the observed data.

240 Table 2 Significance and correlation results of forward multiple linear regression models for the
 241 prediction of THg and MeHg from physiochemical sediment variables; Water Extractable
 242 Organic Carbon (WEOC), pH, Electrical Conductivity (EC), Clay content and Organic Matter
 243 (OM).

Response variable	Fitted terms	F value	R ²
THg	WEOC	61.8***	0.367
	WEOC+pH	48.6***	0.476
	WEOC+pH+EC	35.5***	0.496
	WEOC+pH+EC+Clay	29.9***	0.524
MeHg	EC	7.02**	0.54
	EC+THg	8.36***	0.123
	EC+THg+pH	7.07***	0.148
	EC+THg+pH+Clay	6.05***	0.161
	EC+THg+pH+Clay+WEOC	5.50***	0.176
	EC+THg+pH+Clay+WEOC+OM	6.56***	0.241

244 ** = p < 0.01, *** = p < 0.001

245 The variability in MeHg concentrations was more difficult to explain than the THg
 246 concentrations using the physiochemical variables measured. The multiple linear regression
 247 model for MeHg (Figure 4) had a lower R² value than the model for THg. The fit which included
 248 EC, THg, pH, %Clay, WEOC and %OM (in order of decreasing importance) had an R² value of
 249 0.241 and a p value of < 0.001. Although EC accounted for the greatest extent of the variability
 250 in the MeHg dataset, when considered on its own EC accounted for only 5.4% of the variation.
 251 This indicates that variables that we measured could not adequately explain the concentration of
 252 MeHg in the sediments.



253

254 Figure 4. Total mercury (THg) and methylmercury (MeHg) concentrations observed in
 255 cores sampled from the dyke cell (pre-breach and post-breach) along with adjacent
 256 sites (mudflat and salt marsh) plotted against fitted THg and MeHg concentrations that
 257 were predicted using multiple linear regression models (Table 2) created with the same
 258 data. The THg model included WEOC, pH, EC, and %Clay as explanatory variables,
 259 explaining 51.9% of the variability. The MeHg model included EC, THg, pH, %Clay,
 260 WEOC and %OM as explanatory variables, explaining 24.1% of the variability.

261 **Discussion**

262 *Post-breach sediments are chemically more similar to the salt marsh and mudflat than pre-*
263 *breach sediments*

264 The breaching of the dyke and inundation of the dyke cell deposited a large quantity of fresh
265 sediment over the top of the pre-existing soil. This event changed the biogeochemistry of the
266 system by increasing the EC, pH, %OM and WEOC. The impact of this change is best
267 demonstrated by the considerable increase in the EC observed (Figure 1c) as the dyke cell
268 changed from a terrestrial environment to a coastal environment due to inundation with saline
269 water. While the topography of the mudflat and the salt marsh gently slopes down towards the
270 sea, the soil in the dyke cell was relatively flat prior to breaching and inundation. The deposition
271 of fresh sediment in the dyke cell was unevenly distributed leaving puddles of seawater which
272 we observed in depressed areas at low tide. Evaporation of water and precipitation of salts in
273 these depressed areas (Mouneimne and Price, 2007) has resulted in the EC of the post-breach
274 sediments being elevated above levels measured in the mudflat or the salt marsh (Figure 1c).

275

276 The objective of the managed retreat is for salt marsh vegetation to colonise the freshly deposited
277 sediment once the depth of the sediment raises the wetland to an elevation high enough for
278 vegetation to survive (Williams and Orr, 2002). During the post-breach sampling in 2011 the
279 dyke cell was still unvegetated and looked more similar to a mudflat than a salt marsh. This
280 observation is supported by the textural analysis of the sediment deposited in the dyke cell (post-
281 breach) which was similar to the sediment sampled from the mudflat (Figure 3). The chemistry
282 of the post-breach sediments (WEOC, pH and %OM) was more similar to the salt marsh and

283 mudflat sediments than the samples collected pre-breach. However, this data must be interpreted
284 with caution since only two cores were collected prior to the dyke being breached.

285

286

287 *Post-breach sediments have greater total Hg but lower MeHg concentrations*

288 The total Hg concentrations in the reclaimed region were similar to those found in other studies
289 of non-vegetated intertidal mudflats (O’Driscoll et al., 2011; Sizmur et al., 2013b) and salt
290 marshes (Hung and Chmura, 2006; Sunderland et al., 2004) in the Bay of Fundy. Over a period
291 of two years (and only one year after the dyke was breached) the concentration of total Hg in the
292 dyke cell was considerably greater (Figure 2). We acknowledge, however, that this dataset has
293 limitations since there were only two replicate cores collected prior to the dyke being breached.
294 Despite this apparent increase, the concentration of Hg in the post-breach sediments had not yet
295 reached that of the salt marsh, which is the target ecosystem. There was a clear decrease in Hg
296 concentration with sediment depth in both the mudflat and the post-breach sediments but not in
297 the salt marsh sediments which is a further indication that the sediment characteristics more
298 closely match the mudflat at this stage of restoration.

299

300 While the total Hg concentrations were greater in the dyke cell after inundation, and the MeHg
301 concentrations were greater at the surface of the sediment, MeHg was observed to be lower
302 overall in the post-breach cores (Figure 2). This lower MeHg concentration was reflected by
303 %MeHg in the sediments of the dyke cell decreasing from 6% pre-breach to 2% post-breach
304 when averaged over all the depths. This observation indicates that methylation has not rapidly

305 occurred in the newly deposited Hg(II) species in the sediment. If the lower MeHg in the post-
306 breach sediments was due to greater export of MeHg from the sediments by tidal flushing then
307 we would have expected to see MeHg depleted in the top few cm of sediment. However, MeHg
308 concentrations were greatest in the top few cm (Figure 2). Therefore, tidal flushing is probably
309 not the reason for the lower MeHg in the post-breach sediments.

310

311 Because total Hg concentrations are greater post-breach and MeHg concentrations are lower, Hg
312 methylation cannot be limited by the supply of total Hg. Hg methylation is rather limited by the
313 bioavailability of Hg to Hg methylating bacteria or the activity of these bacteria (Sunderland et
314 al., 2006). Canário et al. (2007) showed that %MeHg in unvegetated coastal wetland sediments
315 were only 0.6%, while vegetated sediments had up to 18% MeHg. The authors explained that
316 this discrepancy is likely to occur because the presence of vegetation increases microbial activity
317 and favours Hg methylation. Colonisation of the dyke cell by benthic invertebrates (e.g.
318 polychaete worms) may also increase the sediment-water interface and the concentration of
319 MeHg in their burrows (Sizmur et al., 2013a). Therefore, the MeHg concentrations in the dyke
320 cell may increase as the restoration progresses and the dyke cell becomes colonised by
321 vegetation and fauna. This prediction must be contrasted with the observation by Morris et al.
322 (2014) that restored salt marshes have lower MeHg concentrations several decades after
323 inundation when compared to adjacent natural salt marshes. It is therefore unclear whether the
324 MeHg concentration in the dyke cell sediments will increase beyond the concentrations in the
325 adjacent natural salt marsh in the long term.

326

327 THg concentrations are influenced by soluble carbon, particle size, pH, and salinity but MeHg
328 concentrations are poorly predicted

329 Water-extractable organic carbon, pH, EC, and clay content of sediments all contributed to the
330 multiple linear regression models that explained 52.4% of the variability associated with the
331 concentration of THg, but only 24% of the variability associated with MeHg concentrations in
332 the sediments (Table 2 and Figure 4). Clay content was positively correlated with THg sediment
333 concentration. A reduction in sediment particle size (here observed by an increase in clay
334 content) increases the surface-area-to-volume ratio of particulates in a system. The high surface
335 area and cation exchange capacity of clays results in the adsorption of Hg to fine particles
336 (Bengtsson and Picado, 2008). Suspension of fine sediments in the tidal water increases the
337 likelihood of sediments to scavenge Hg from the water column by settling and retaining Hg in
338 the accumulating sediment (Covelli et al., 2009; Hung and Chmura, 2006; Sunderland et al.,
339 2006). Sediments comprised of fine particles also increase the proportion of particle-bound Hg
340 (Bengtsson and Picado, 2008) and may thus reduce the bioavailability of Hg to methylating
341 bacteria.

342

343 Dissolved organic matter (DOM) is a major binding phase for Hg in aquatic environments
344 (Haitzer et al., 2002; Haverstock et al., 2012; Le Faucheur et al., 2014; O'Driscoll and Evans,
345 2000; Ravichandran, 2004). Here we use WEOC as a proxy for DOM in the sediments following
346 Sizmur et al (2013b). Although we found a positive correlation between THg and both %OM and
347 WEOC, the WEOC explains the THg concentration in the sediments better (Table 2). This
348 observation indicates that the changes in Hg in the sediments are due to a greater fraction that is
349 bound to soluble carbon complexes. The concentration of WEOC in the post-breach sediments

350 (Figure 3) was higher than the mudflat and (unlike the salt marsh) was not associated with
351 vegetation growing in situ. It is therefore likely that the cause of higher concentrations of WEOC
352 (and THg) in the post-breach sediments, compared to the mudflat, is the decaying mat of
353 terrestrial vegetation underneath the freshly deposited sediment. Hg complexation with DOM
354 reduces the bioavailability of Hg to methylating bacteria because the complexes are generally too
355 large to penetrate their biological membranes (Le Faucheur et al., 2014; Ravichandran, 2004).
356 However, soluble organic matter also provides an energy source for methylating bacteria and
357 may increase their activity resulting in greater methylation rates (Ullrich et al., 2001). Further
358 increases in DOM (and microbial activity) are likely to occur as the dyke cell becomes vegetated
359 (Canário et al., 2007) which may increase methylation rates in the future. The deposition of
360 plankton is likely to increase the %MeHg in the fresh sediment as they contain approximately
361 6% to 15% MeHg in the Northwest Atlantic Ocean (Hammerschmidt et al., 2013).

362

363 The solubility and speciation of Hg and the binding of dissolved Hg species to DOM or sediment
364 particles is pH dependent (Gabriel and Williamson, 2004). At low pH, H^+ competes with Hg for
365 binding sites on DOM or the surface of sediment particles, which releases Hg into solution but
366 they also both compete for uptake by negatively charged bacterial cells. In this study pH
367 correlated positively with Hg but negatively with MeHg. This contrast indicates that the greater
368 pH of the mudflat, salt marsh, and post-breach sediments, compared to pre-breach sediments
369 (Figure 3) resulted in greater Hg retention (Hung and Chmura, 2006) but may have reduced Hg
370 bioavailability to methylating bacteria (Barkay et al., 1997; Gilmour and Henry, 1991; Le
371 Faucheur et al., 2014).

372

373 The increase in EC that resulted from the inundation of the dyke cell with sea water (Figure 1c)
374 is due to the high salinity of the seawater (Mouneimne and Price, 2007). The high salinity of the
375 sediment deposited after the dyke cell was inundated with seawater created an environment with
376 a higher ionic strength. As ionic strength increases, the concentration of Hg desorbed into
377 solution decreases (Duarte et al., 1991) resulting in greater Hg retention in sediments and a
378 decrease in the bioavailability of Hg to methylating bacteria (Barkay et al., 1997). Seawater
379 contains high concentrations of chloride ions which can form strong ($\log_{10} K_1^\circ = 7.31$)
380 complexes with mercury species (Powell et al., 2005). The greater the concentration of chloride,
381 the more negatively charged mercuric chloride ions (HgCl_3^- and HgCl_4^{2-}) will be present in
382 solution and these negative ions also have a lower bioavailability (Barkay et al., 1997) to
383 methylating bacteria with negatively charged cell walls. Therefore, the increase in ionic strength
384 and formation of trivalent or tetravalent mercuric chloride species in the high EC sediments of
385 the post-breach sediments may have reduced their bioavailability to mercury methylating
386 bacteria. These Hg-chloride complexes may also be less susceptible to photoreduction and loss to
387 the atmosphere (Qureshi et al., 2009).

388

389 In summary, the chemical changes that occur in the sediment after inundation may have
390 impacted on the bioavailability of Hg to methylating bacteria. The decrease in particle size
391 distribution and subsequent increase in sediment surface area may have increased sorption of Hg
392 out of the water column but lowered its bioavailability. Higher organic matter levels may provide
393 a food source for methylating bacteria and increase their activity. Greater soluble organic carbon
394 may mobilise Hg from the surface of sediments but also complex it in a form that is unavailable
395 to methylating bacteria. An increase in sediment pH increases the concentration that can be

396 adsorbed from the solution phase and reduces the bioavailability. Finally, the higher ionic
397 strength leads to a greater proportion of inorganic complexes and a lower bioavailability of Hg.
398 This final conclusion assumes that the uptake of Hg by methylating bacteria occurs by passive
399 diffusion of neutral or ionic lipophilic Hg species but there is now a considerable body of
400 evidence to suggest that uptake may occur by facilitated diffusion or active transportation by
401 protein pumps (Hsu-Kim et al., 2013).

402

403 *Conclusions and Implications for Coastal Managed Retreat*

404 Despite a doubling of Hg concentration within the dyke cell after the dyke was breached, Hg
405 concentrations are still below the Canadian Sediment Quality Guidelines (CCME, 2002). The
406 reason for the Hg increase in this study was the fresh deposition of sediments with a smaller
407 particle size distribution that are able to scavenge and retain Hg due to their higher surface area,
408 negative charge, and higher pH. This site can therefore be considered a net sink for mercury
409 during the first year after the dyke was breached. The more sediment that is deposited, the larger
410 the sink will become. In contrast to considerable increases in mercury methylation observed
411 during freshwater wetland creation (Kelly et al., 1997; Sinclair et al., 2012), we observed a 27%
412 decrease in MeHg concentrations in the dyke cell after the dyke was breached. This decrease
413 may have been due to greater Hg retention and lower Hg bioavailability to methylating bacteria
414 but ultimately cannot be fully explained with the available data and is limited by the low number
415 of replicate cores collected. Further work will be required to explain the precise mechanisms for
416 this decrease.

417

418 Our data provides no evidence for a flush of Hg methylation during the first year of managed
419 retreat. As the restoration progresses and vegetation colonises, the soluble carbon concentration
420 and microbial activity may increase and the rate of Hg methylation may also increase. However,
421 contradictory data from other studies indicate that it is unclear whether MeHg will be elevated
422 beyond the concentration found in natural wetlands (Canário et al., 2007; Kelly et al., 1997;
423 Morris et al., 2014; Sinclair et al., 2012). We conclude that coastal flooding of sediments subject
424 to diffuse Hg contamination during managed retreat of coastal flood defences does not pose a
425 significant risk of increasing Hg methylation or bioavailability during the first year.

426

427 **Acknowledgements**

428 Financial support for this research was provided by the Canada Research Chairs, the Ducks
429 Unlimited Canada - Acadia University Partnership Grant, and an NSERC Discovery Grant
430 awarded to NJO.

431

432 **References**

- 433 Barkay, T., Gillman, M., Turner, R.R., 1997. Effects of dissolved organic carbon and salinity on
434 bioavailability of mercury. *Applied and environmental microbiology* 63, 4267-4271.
- 435 Bengtsson, G., Picado, F., 2008. Mercury sorption to sediments: Dependence on grain size,
436 dissolved organic carbon, and suspended bacteria. *Chemosphere* 73, 526-531.
- 437 Byers, S.C., Mills, E.L., Stewart, P.L., 1978. A comparison of methods of determining organic
438 carbon in marine sediments, with suggestions for a standard method. *Hydrobiologia* 58, 43-47.
- 439 Canário, J., Caetano, M., Vale, C., Cesário, R., 2007. Evidence for elevated production of
440 methylmercury in salt marshes. *Environmental science & technology* 41, 7376-7382.

441 CCME, 2002. Canadian Sediment Quality Guidelines for the Protection of Aquatic Life.

442 Compeau, G., Bartha, R., 1985. Sulfate-reducing bacteria: principal methylators of mercury in
443 anoxic estuarine sediment. *Applied and environmental microbiology* 50, 498-502.

444 Covelli, S., Acquavita, A., Piani, R., Predonzani, S., De Vittor, C., 2009. Recent contamination
445 of mercury in an estuarine environment (Marano lagoon, Northern Adriatic, Italy). *Estuarine,
446 Coastal and Shelf Science* 82, 273-284.

447 Crowell, N., Webster, T., O'Driscoll, N.J., 2011. GIS modelling of intertidal wetland exposure
448 characteristics. *Journal of Coastal Research* 27, 44-51.

449 Desplanque, C., Mossman, D.J., 2004. Tides and their seminal impact on the geology,
450 geography, history, and socio-economics of the Bay of Fundy, eastern Canada. *Atlantic Geology*
451 40.

452 Duarte, A., Pereira, M., Oliveira, J., Hall, A., 1991. Mercury desorption from contaminated
453 sediments. *Water Air & Soil Pollution* 56, 77-82.

454 Emmerson, R., Birkett, J., Scrimshaw, M., Lester, J., 2000. Solid phase partitioning of metals in
455 managed retreat soils: field changes over the first year of tidal inundation. *Science of the Total
456 Environment* 254, 75-92.

457 Evers, D.C., Han, Y.-J., Driscoll, C.T., Kamman, N.C., Goodale, M.W., Lambert, K.F., Holsen,
458 T.M., Chen, C.Y., Clair, T.A., Butler, T., 2007. Biological mercury hotspots in the northeastern
459 United States and southeastern Canada. *Bioscience* 57, 29-43.

460 Gabriel, M.C., Williamson, D.G., 2004. Principal biogeochemical factors affecting the speciation
461 and transport of mercury through the terrestrial environment. *Environmental geochemistry and
462 health* 26, 421-434.

463 Gilmour, C.C., Henry, E.A., 1991. Mercury methylation in aquatic systems affected by acid
464 deposition. *Environmental Pollution* 71, 131-169.

465 Gordon Jr, D.C., Baretta, J.W., 1982. A preliminary comparison of two turbid coastal
466 ecosystems: The Dollard (Netherlands-FRG) and the Cumberland Basin (Canada).
467 *Hydrobiological Bulletin* 16, 255-267.

468 Guédron, S., Huguet, L., Vignati, D., Liu, B., Gimbert, F., Ferrari, B., Zonta, R., Dominik, J.,
469 2012. Tidal cycling of mercury and methylmercury between sediments and water column in the
470 Venice Lagoon (Italy). *Marine Chemistry* 130, 1-11.

471 Haitzer, M., Aiken, G.R., Ryan, J.N., 2002. Binding of mercury (II) to dissolved organic matter:
472 the role of the mercury-to-DOM concentration ratio. *Environmental science & technology* 36,
473 3564-3570.

474 Hammerschmidt, C.R., Finiguerra, M.B., Weller, R.L., Fitzgerald, W.F., 2013. Methylmercury
475 accumulation in plankton on the continental margin of the northwest atlantic ocean.
476 *Environmental science & technology* 47, 3671-3677.

477 Haverstock, S., Sizmur, T., Murimboh, J., O'Driscoll, N.J., 2012. Modeling the photo-oxidation
478 of dissolved organic matter by ultraviolet radiation in freshwater lakes: Implications for mercury
479 bioavailability. *Chemosphere* 88, 1220-1226.

480 Heim, W.A., Coale, K.H., Stephenson, M., Choe, K.-Y., Gill, G.A., Foe, C., 2007. Spatial and
481 habitat-based variations in total and methyl mercury concentrations in surficial sediments in the
482 San Francisco Bay-Delta. *Environmental science & technology* 41, 3501-3507.

483 Hsu-Kim, H., Kucharzyk, K.H., Zhang, T., Deshusses, M.A., 2013. Mechanisms Regulating
484 Mercury Bioavailability for Methylating Microorganisms in the Aquatic Environment: A Critical
485 Review. *Environmental science & technology* 47, 2441-2456.

486 Hung, G.A., Chmura, G.L., 2006. Mercury accumulation in surface sediments of salt marshes of
487 the Bay of Fundy. *Environmental Pollution* 142, 418-431.

488 Kelly, C., Rudd, J., Bodaly, R., Roulet, N., St. Louis, V., Heyes, A., Moore, T., Schiff, S.,
489 Aravena, R., Scott, K., 1997. Increases in fluxes of greenhouse gases and methyl mercury
490 following flooding of an experimental reservoir. *Environmental science & technology* 31, 1334-
491 1344.

492 Lavoie, R.A., Hebert, C.E., Rail, J.-F., Braune, B.M., Yumvihoze, E., Hill, L.G., Lean, D.R.,
493 2010. Trophic structure and mercury distribution in a Gulf of St. Lawrence (Canada) food web
494 using stable isotope analysis. *Science of the Total Environment* 408, 5529-5539.

495 Le Faucheur, S., Campbell, P.G.C., Fortin, C., Slaveykova, V.I., 2014. Interactions between
496 mercury and phytoplankton: Speciation, bioavailability, and internal handling. *Environmental*
497 *Toxicology and Chemistry* 33, 1211-1224.

498 Miller, W., Miller, D., 1987. A micro-pipette method for soil mechanical analysis.
499 *Communications in Soil Science & Plant Analysis* 18, 1-15.

500 Morris, M.A., Spencer, K.L., Belyea, L.R., Branfireun, B.A., 2014. Temporal and spatial
501 distributions of sediment mercury in restored coastal saltmarshes. *Marine Chemistry* 167, 150-
502 159.

503 Mouneimne, S.M., Price, J.S., 2007. Seawater contamination of a harvested bog: hydrological
504 aspects. *Wetlands* 27, 355-365.

505 O'Driscoll, N.J., Evans, R.D., 2000. Analysis of methyl mercury binding to freshwater humic
506 and fulvic acids by gel permeation chromatography/hydride generation ICP-MS. *Environmental*
507 *science & technology* 34, 4039-4043.

508 O'Driscoll, N.J., Canário, J., Crowell, N., Webster, T., 2011. Mercury speciation and distribution
509 in coastal wetlands and tidal mudflats: relationships with sulphur speciation and organic carbon.
510 *Water, Air, & Soil Pollution* 220, 313-326.

511 Ollerhead, J., Spicer, C., Bams, R., 2011. Monitoring a salt marsh restoration at Fort Beausejour,
512 Aulac, NB - Final Report, Ducks Unlimited Canada.

513 Portnoy, J., Giblin, A., 1997. Effects of historic tidal restrictions on salt marsh sediment
514 chemistry. *Biogeochemistry* 36, 275-303.

515 Powell, K.J., Brown, P.L., Byrne, R.H., Gajda, T., Hefter, G., Sjöberg, S., Wanner, H., 2005.
516 Chemical speciation of environmentally significant heavy metals with inorganic ligands. Part 1:
517 The Hg^{2+} - Cl^- , OH^- , CO_3^{2-} , SO_4^{2-} , and PO_4^{3-} -aqueous systems (IUPAC Technical Report).
518 *Pure and applied chemistry* 77, 739-800.

519 Qureshi, A., O'Driscoll, N.J., MacLeod, M., Neuhold, Y.-M., Hungerbühler, K., 2009.
520 Photoreactions of mercury in surface ocean water: gross reaction kinetics and possible pathways.
521 *Environmental science & technology* 44, 644-649.

522 Rasmussen, R.S., Nettleton, J., Morrissey, M.T., 2005. A review of mercury in seafood: Special
523 focus on tuna. *Journal of Aquatic Food Product Technology* 14, 71-100.

524 Ravichandran, M., 2004. Interactions between mercury and dissolved organic matter—a review.
525 *Chemosphere* 55, 319-331.

526 Sinclair, K.A., Xie, Q., Mitchell, C.P., 2012. Methylmercury in water, sediment, and
527 invertebrates in created wetlands of Rouge Park, Toronto, Canada. *Environmental Pollution* 171,
528 207-215.

529 Singh, K., Walters, B.B., Ollerhead, J., 2007. Climate change, sea-level rise and the case for salt
530 marsh restoration in the Bay of Fundy, Canada. *Environments: a journal of interdisciplinary*
531 *studies* 35.

532 Sizmur, T., Canário, J., Edmonds, S., Godfrey, A., O'Driscoll, N.J., 2013a. The polychaete worm
533 *Nereis diversicolor* increases mercury lability and methylation in intertidal mudflats.
534 *Environmental Toxicology and Chemistry* 32, 1888-1895.

535 Sizmur, T., Canário, J., Gerwing, T.G., Mallory, M.L., O'Driscoll, N.J., 2013b. Mercury and
536 methylmercury bioaccumulation by polychaete worms is governed by both feeding ecology and
537 mercury bioavailability in coastal mudflats. *Environmental Pollution* 176, 18-25.

538 Sizmur, T., Palumbo-Roe, B., Hodson, M.E., 2011. Impact of earthworms on trace element
539 solubility in contaminated mine soils amended with green waste compost. *Environmental*
540 *Pollution* 159, 1852-1860.

541 Sunderland, E.M., Amirbahman, A., Burgess, N.M., Dalziel, J., Harding, G., Jones, S.H., Kamai,
542 E., Karagas, M.R., Shi, X., Chen, C.Y., 2012. Mercury sources and fate in the Gulf of Maine.
543 *Environmental research* 119, 27-41.

544 Sunderland, E.M., Gobas, F.A., Branfireun, B.A., Heyes, A., 2006. Environmental controls on
545 the speciation and distribution of mercury in coastal sediments. *Marine Chemistry* 102, 111-123.

546 Sunderland, E.M., Gobas, F.A., Heyes, A., Branfireun, B.A., Bayer, A.K., Cranston, R.E.,
547 Parsons, M.B., 2004. Speciation and bioavailability of mercury in well-mixed estuarine
548 sediments. *Marine Chemistry* 90, 91-105.

549 U.S.EPA, 1998. Method 7473: Mercury in solids and solutions by thermal decomposition,
550 amalgamation and atomic spectrophotometry, U.S. Environmental Protection Agency,
551 Washington, DC.

552 Ullrich, S.M., Tanton, T.W., Abdrashitova, S.A., 2001. Mercury in the aquatic environment: a
553 review of factors affecting methylation. *Critical Reviews in Environmental Science and*
554 *Technology* 31, 241-293.

555 Williams, P.B., Orr, M.K., 2002. Physical evolution of restored breached levee salt marshes in
556 the San Francisco Bay estuary. *Restoration Ecology* 10, 527-542.

557 Wynn, G., 1979. Late eighteenth-century agriculture on the Bay of Fundy marshlands.
558 *Acadiensis*, 80-89.

559

560